

Effect of ECAP Routes on Mechanical Properties and Microstructure of AA6061-T4 recycled chips

Research Paper

Prepared by:

Rawa Hamza Mohammed

26/2/2024

Corresponding author: E-mail address: rawa.hamza.m@spu.edu.iq;

ORCID ID: <https://orcid.org/0000-0003-2618-9633>

Keywords: ECAP; SEM; Route; Fractography; Mechanical properties.

List of Contents

List of Contents	2
List of Figures	3
List of Tables	3
List of Abbreviations	4
Abstract	5

Sections

1. Introduction	6
2 Experimental	11
2.1 Material and Equipment	11
2.2 Preparation of the Experimental Work	12
3. Results and Discussion	16
3.1 Influence Routes on tensile strength	16
3.2 Impact of Routes on Hardness	20
3.3 Influence of Routes on Microstructures	20
3.4 Comparisons between the previous studies with the current study	24
4. Conclusion	26
5. References	27

List of Figures

Figure No.	Title of the Figure	Page No.
Figure 1	Demonstrated various configurations of the experimental work setup.	12
Figure 2	Experimental diagram (Methodology)	13
Figure 3	Display the ECAP Die (a) demonstrating the ECAP Die (b) showcasing the two-piece split die component.	15
Figure 4	Figure 4: Depiction of (a) Schematic representation of ECAP routes BC and C inducing rotations around the longitudinal axis X of the billet by +90° and 180° respectively (b) Orientation of X, Y, and Z axes (on the left) and planes (on the right)	15
Figure 5	Final products of solid-state recycling of AA6061-T4 alloy recycled chips	16
Figure 6	The dimensions of the tensile test samples are expressed in (mm)	17
Figure 7	Representation of tensile specimens (a) specimens before tensile testing (b) specimens after tensile examination	17
Figure 8	Different fractured specimens were seen using SEM (a) Received material brittle-ductile fracture (b) Extruded sample, (c) 4 th route C ECAP specimen and (d) 4 th route BC ECAP specimen displaying shear rupture	23

List of Tables

Table No.	Title of the table	Page No.
Table 1	Chemical Compositions of AA6061-T4 aluminum alloy	11
Table 2	Mechanical Properties of AA6061-T4 aluminum alloy	12
Table 3	Mechanical properties of AA6061-T4 before and after ECAP using Route BC	19
Table 4	Mechanical properties of AA6061-T4 before and after ECAP using Route C	19
Table 5	A comparisons between the previous studies with the current study in terms of ultimate tensile strength, elongation to failure, and micro-hardness	25

Abbreviation's List	Description
ECAP	Equal channel angular pressing
RT-ECAP	Room Temperature –Equal channel angular pressing
I-ECAP	Incremental - Equal channel angular pressing
Φ	Angle of intersection of two channel Die (Die inner angle)
Ψ	Outer arc angle of Die (Die corner angle)
ϵ	Strain
R	Extrusion ratio
BC	Type of route of ECAP process
C	Type of route of ECAP process
SPD	Severe plastic deformation
UTS	Ultimate tensile strength
Y.S	Yield strength
S.S.R	Solid State Recycling
H.V	Unit of micro hardness
$^{\circ}\text{C}$	Unit of temperature (Celsius)
MPa	Unit of strength (pressure)
m/min	Cutting speed
mm	Depth of cut
Mm/rev	Feed
bar	Unit of pressure (hydrostatic compressive stress)
\emptyset	Diameter of bar in mm
MoS ₂	Molybdenum disulfide
UTM	Universal testing machine
EDM	Electro Discharge Machine
ASTM	American Society for Testing and Materials

Abstract

Aluminum alloy finds strong suitability in industries such as automotive, sporting, goods aerospace, and weight reduction. Its blend of lightweight attributes and robust strength make it well-suited for crafting lightweight components and structures while upholding overall strength and performance standards. In this research, AA6061-T4 alloy chips underwent a recycling process involving hot extrusion followed by Equal Channel Angular Pressing. The influence of various routes and varied numbers of cycles on microstructure and mechanical characteristics were examined utilizing a die featuring angles of 90° and 20° . Two routes, BC and C, were scrutinized, and the outcomes displayed significant enhancements in properties for the recycled chips subsequent to the hot extruded and ECAP techniques. After fourth run, route BC exhibited a maximum Ultimate tensile strength of 265 MPa peak yield strength of 149 MPa, and an elongation to failure of 46%. Meanwhile, for route C the corresponding values were 238 MPa 136 MPa, and 41%, respectively. For two routes, BC and C, every pass led to elevated strength and hardness while also contributing to increased elongation to failure. The microstructures and mechanical characteristics of the ECAPed samples surpassed those of the extruded sample. The routes and pass numbers played a substantial role in impacting the microstructures and mechanical properties of the solid-state recycled AA6061-T4 alloy chip specimens. Scanning electron microscopy pictures showcased a honeybee-type pattern following ECAP through route BC, signifying the final stages of grain refinement, while the initial sample exhibited a fracture tendency with a mix of brittleness and ductility.

1. Introduction

Aluminum alloy stands as a widely employed aluminum alloy across diverse industries, recognized for its balanced strength, heat treatability, weld-ability, formability, resistance to corrosion, encompassing, machinability, exceptional characteristics, and lightweight properties. Its affordability further contributes to its popularity among aluminum, manufacturing entities. This alloy finds extensive usage in sectors including furniture manufacturing, irrigation applications, agriculture fitting production, marine structures pipe, aerospace, and automotive [1].

The demand for aluminum is projected to sustain its upward trajectory owing to its favorable attributes, which encompass elevated strength, lightweight nature, exceptional conductivity, and resistance to corrosion. In contrast to conventional aluminum recycling techniques involving remelting, the practice of solid-state recycling through plastic deformation presents noteworthy advantages. These advantages encompass diminished expenses, reduced power consumption, and a streamlined operational process [2]. The elongated, slender, and spiral configuration of aluminum chips renders the conventional remelting recycling approach unfavorable due to notable metal waste. Furthermore; additional losses are incurred at each successive treatment phase, leading to a maximum recovery of only fifty-four percent of the materials through traditional re-melting and recycling procedures [3].

Several scientists [4] have acknowledged the exceptional plastic deformation achieved via hot extrusion when contrasted with alternative methods. The capacity to subject compressed chips to substantial plastic deformation renders it a compelling and auspicious avenue for recycling. In its present characterization, Severe Plastic

Deformation (SPD) encompasses any metal forming technique that employs elevated hydrostatic pressure to induce substantial strain within a bulk solid.

This process leads to remarkable grain refinement while maintaining negligible alterations in overall dimensions [5, 6]. New approaches to severe plastic deformation have been developed, including high-pressure torsion (HPT) [7], multi-directional forging (MDF) [8], cyclic extrusion compression (CEC) [9], accumulative roll bonding (ARB) [10], dissimilar channel angular pressing (DCAP) [11], equal channel angular pressing (ECAP) [12], among others. Among these techniques for producing ultrafine-grained materials, severe plastic deformation (SPD) technologies such as ECAP and torsion straining have proven to be particularly advantageous.

Equal channel angular pressing stands as one of the most extensively employed severe plastic deformation methods for enhancing the strength of lightweight alloys. The SPD technique is introduced as an effective method for enhancing material strength through the conversion of coarse grains into structures characterized by ultrafine-grained (UFG) morphology [13].

In addition, J. R. Duflou et al. [14] researched the ecological influence of the Solid-state recycling (S.S.R.) technique to produce net-form items with little to no pollution while seeking to extend the solid-state recycling process to produce goods suitable for producing other commodities.

The growing significance of S.S.R. by extrusion or different techniques starting with solid state chips has been encouraged by B. Wan et al. [3] and additional prior investigation about enhancing solid-state recycling within extrusion employing frictional-

stir extrusion by D. Baffari et al. [15] Extrusion or other techniques that started with “solid-state” chips have increased the relevance of solid-state recycling. W. Maziarz et al. [16]. An investigation was conducted to examine the morphology and mechanical features of composites through TCAP at 350°C, 400°C, and 450°C. The finding yielded a composite with a matrix comprising equiaxed grains of varying sizes contingent upon the process temperature and particles measuring around 1µm in diameter exhibiting a twinned structure. The process of dynamical recrystallization significantly influenced the specimens, hardness leading to a decrease in hardness levels.

Employing a die with the optimum design factors, the mechanical properties of the AA6063 alloy were examined both before and after the ECAP technique by K. Mohan Agarwal et al. [17]. Applying a die via an angle die with two intersected channels at 90, and 20 degrees, an examination was conducted. Tensile strength rose with each run, but elongation was marginally reduced, as indicated by the stress-strain graph.

The study focused on analyzing the influence of morphology in AA5083 alloy following equal channel angular pressing treatment conducted at both room temperature and elevated temperatures by M. Baig et al. [18]. After undergoing three runs, strength demonstrated an increase to 251 MPa at a temperature of 250 °C.

The study delved into investigating the deformation behavior of a magnesium alloy by P. C. Gautam et al. [19]. The findings indicated that as grain refinement occurs, there is an increase in yield strength while, ultimate compressive strength (UCS) and strain to failure witness a decrease. The grain size significantly influences the strain-hardening behavior at ambient temperatures.

The morphology of the AA6060 alloy revealed the presence of a fragmented grain structure, according to M. Lefstad et al. [20] Applying a die via an angular with 2 channels crossing at 90° and 20.2° degrees, the investigation was carried out through the BC route. Effects of combined ECAP and HPT processes on received material tribology characteristics, mechanical properties, and morphology improvement by M. Ibrahim et al. [21].

The findings indicated an upward trend in tensile strength along with a reduction in elongation as the number of ECAP passes and HPT revolutions increased. This behavior was attributed to grain refinement. Furthermore, the dominant mode of tensile fracture, across all samples was found to be shear fracture with a decline in the shear angle evident with greater imposed strain. The dimple size exhibited a significant decrease, with an increase in the number of ECAP passes and HPT revolutions corresponding to the decrease in grain size.

The tensile properties of AA6063 alloy were improved by O.P. Abioye et al. [22]. Extruding set A of the samples' billets into the die once was how the procedure was performed. According to the research, aluminum alloys are always strengthened by using ECAE. Both the elongation to failure (twenty-nine percent) and the Young Modulus 11GPa after four cycles were recorded. Surprisingly, M.I.Ab Kadir et al. [23] applied hot compact (homogenization) to AA and Mg chip samples prior to extrusion at different preheating temperatures periods extending from twenty minutes to six hours.

AA6061 alloy chips were recycled by M. A. Taha et al. [24]. Using a die with a 90° angle. For six cycles, the hardness increased to 85 HV after the combination of extrusion with ECAP, as observed. Investigation revealed that the sample grain sizes

diminished by 5, 3.28, and 2.46 μm during each of the 2, 4, and 6 runs, significantly. Structural evolution, mechanical, and physical features of samples made of AA6061 alloy. The effects of extruded ratio and extruded temperatures were examined by M.I. Abd et al. [25] Samples with ER12.8 and ET at ET500 $^{\circ}\text{C}$ show better mechanical characteristics than the original ones. The last twenty years have seen a rise in the significance of hot extrusion as a technique for reutilization, which culminated in the most recent efforts by J. Liang et al. [26].

As stated by J. Gronostajski et al. [27] claim that a specific amount of ϵ is necessary to remove layers of oxide from chip surfaces and produce a clean surface of metal as an outcome of improving the bond. Investigation of the effects of cracking plane orientations on the test of fatigue cracking development rates and fracturing resistance of AA6063 by M. Ali Kazemi et al. [28].

A die with 90 $^{\circ}$ and 22 $^{\circ}$ angles was employed for the study. The outcomes demonstrated a significant enhancement in UTS, increasing to 209 MPa accompanied by a reduction in the average grain size from 45 μm to approximately 230nm after undergoing four cycles. Al and Mg alloy types are extensively utilized in applications in structure owing to their remarkable mechanical features and amalgamation of lightweight attributes. Many sectors of industries, including furniture, automobile, plumbing, and other products, commonly use AA6061 alloy water for agricultural purposes [29].

ECAP has proven to be an efficient method for refining bulk metal and converting coarse grain structures into materials with excellent mechanical properties. As a result, it has been utilized in the solid-state recycling of aluminum machining chips to produce products with enhanced characteristics. One area that shows promise is the combination

of hot extrusion followed by ECAP at ambient temperature, which has demonstrated more effective results due to the improved morphology of the materials. Additionally, this approach requires less energy compared to using a higher-temperature version of the same process to create high-strength materials. However, there is a lack of experimental investigations in this specific area based on the authors' knowledge. In order to build upon existing studies, the selection of ECAP process factors for the present investigation, along with their impact on mechanical properties and morphology, was carefully considered to yield the most desirable outcomes from the research.

2. Experimental

2.1 Material and Equipment

A Figure 1 and 2 illustrates the arrangement and setup used for the experimental work. This study employed the industrially available AA6061 alloy. Physical characteristics, mechanical properties, and chemical composition are detailed in Tables 1 and 2.

Table 1: Chemical Compositions of AA6061-T4 aluminum alloy

Chemical Compositions										Base
Elements	Mg	Si	Fe	Cu	Mn	Cr	Zn	Ti	Others	Al
%Min	0.8	0.4	-	0.15	-	0.04	-	-		95.8
%Max [1, 30]	1.2	0.8	0.7	0.4	0.15	0.35	0.25	0.15	0.15	98.6
AA6061-T4	0.92	0.60	0.26	0.23	0.15	0.12	0.03	0.013	0.115	97.562

Table 2: Mechanical Properties of AA6061-T4 aluminum alloy [1, 30]

Property	AA6061-T4
Tensile Strength	250 MPa 36000 psi
Yield Strength	110 MPa 16000 psi
Micro- hardness	81.66 HV
Elongation	27%
Density	2.70 g/cc 0.0975 lb/in ³

2.2 Preparation of the Experimental Work.

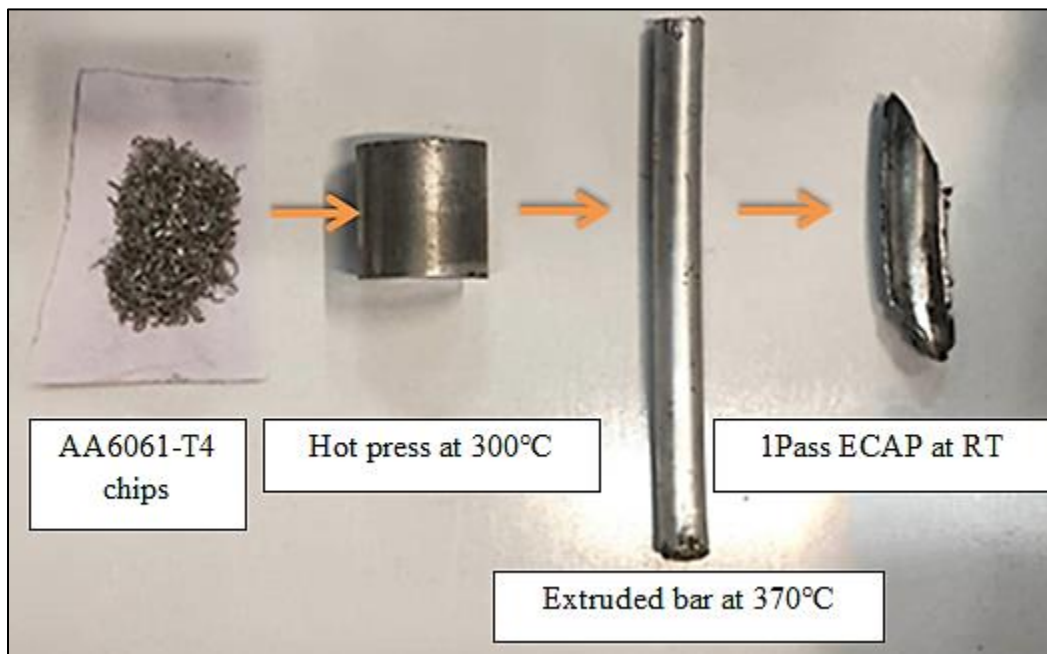


Figure 1: Demonstrated various configurations of the experimental work setup.

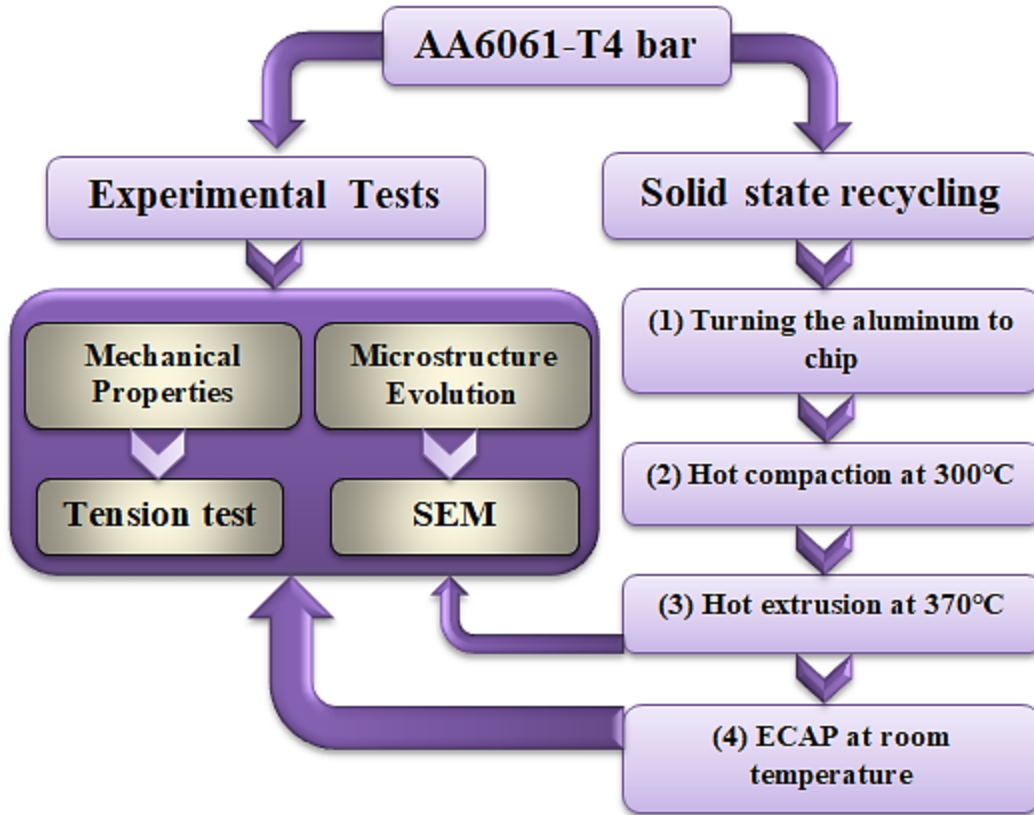


Figure 2: Experimental diagram (Methodology).

In the current study, the original bar stock was dry-turned to create AA6061-T4 alloy chips. The machining process utilized the subsequent cutting parameters a cutting speed of 88 m/min, a depth of cut set at 1 mm, and a feed rate of 1 mm/rev [25]. The chips underwent compaction at a temperature of 300 °C. The compacted sample possessed dimensions of $\varnothing= 45 \times 80$ mm, and a compressive force of 200 bar was applied during this stage. Subsequently; extrusion was conducted at 370 °C through a cone-shaped die with an extrusion ratio of 9 (approximately $\varepsilon = 2$).

This process was carried out using a horizontal hydraulic press with a capacity of 200 tons, and a speed of 10mm/s, while the extrusion compressive force was maintained at 100 bar. As a result, intermediate items with a diameter of Φ 15 mm were successfully

produced. The utilization of hot extrusion, characterized by intense compressive, and shear forces at elevated temperatures, was employed to achieve comprehensive strengthening of the compacted recycled material chips [31]. Cylindrical samples with a diameter of $\text{Ø} 15$ mm and a length of 60 mm designed as billets were machined from the extruded samples.

The ECAP process was carried out using a two-part divided die configuration, as illustrated in Figure 3. The die material employed was tool steel, chosen for its suitability in reducing process time as it doesn't require bolts. The channels within the die intersected at an angle of $\Phi = 90^\circ$, while the outer corner angle was $\Psi = 20^\circ$. To optimize grain refinement and enhance mechanical properties, process was conducted through two selected routes: BC and C. The choice of these routes was based on recommendations mentioned in the references [32, 33].

Equal Channel Angular Pressing was implemented on billets with dimensions of $\text{Ø}15 \times 50$ mm. The procedure ensured a consistent strain of approximately 1.05 in each successive run [6]. Samples were subjected to significant simple shear strains [34]. The study explored the control of varying numbers of passes (1, 2, 4) using different routes at ambient temperature, as depicted in Figure 4. Among these routes, Route BC was identified as the most efficient for creating ultrafine-grained (UFG) materials with consistent morphology. The process involved employing a vertical hydraulic press (Model CH-250x250) with a 100-ton capacity operating at a pressing speed of 10 mm/min [35]. In this process, for each pressing stage, molybdenum disulfide (MoS_2) was employed as a lubricant [32, 33].

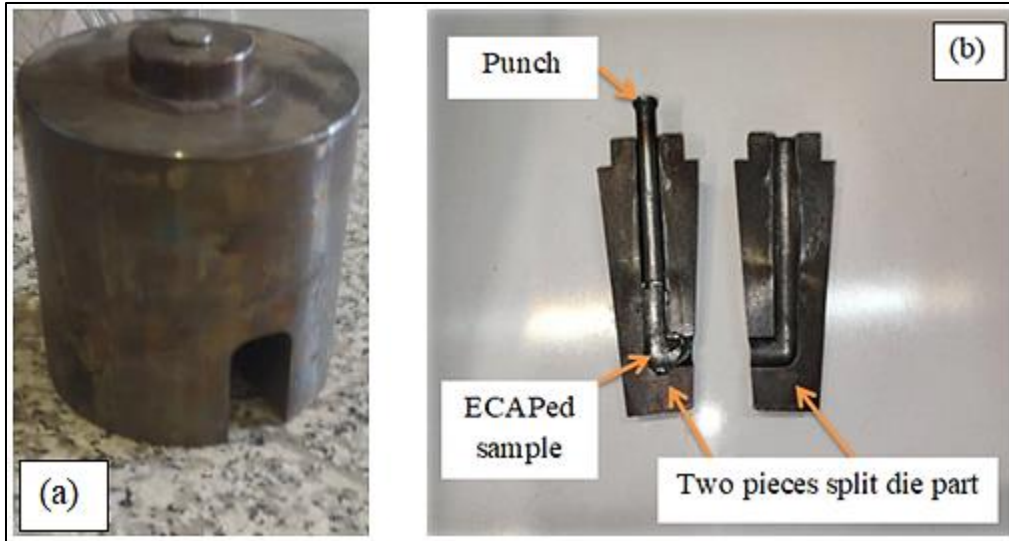


Figure 3: Display the ECAP Die (a) demonstrating the ECAP Die (b) showcasing the two-piece split die component.

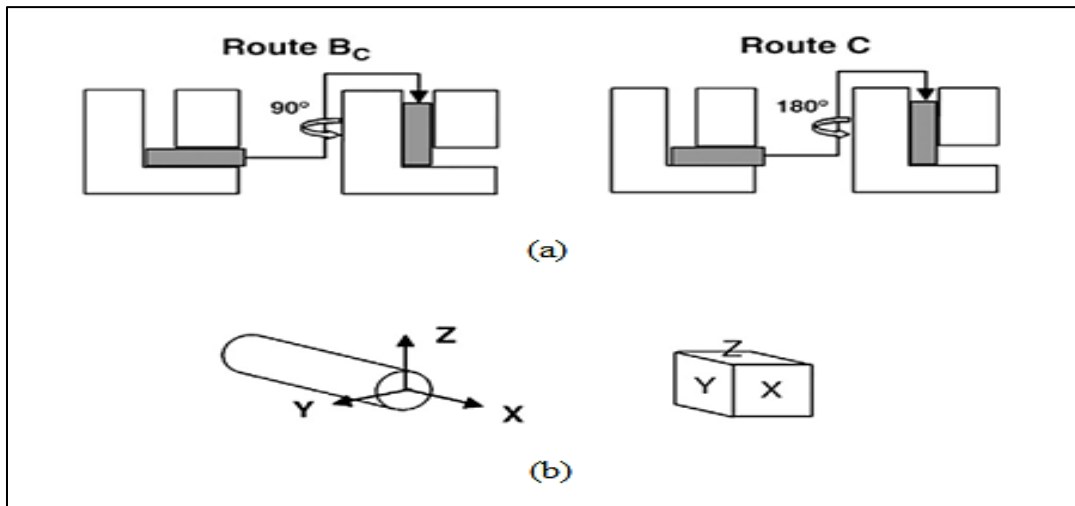


Figure 4: Depiction of (a) Schematic representation of ECAP routes BC and C inducing rotations around the longitudinal axis X of the billet by $+90^\circ$ and 180° respectively (b) Orientation of X, Y, and Z axes (on the left) and planes (on the right) [32, 33].

The procedure of ECAP was implemented on billets with 4 cycles at RT. During the process, samples were pressed at a speed of 10 mm/s. utilizing a vertical hydraulic press of 100 tons. According to ECAP technology, the level of plastic strain is around 1.05 in

each cycle [36]. The samples were subjected to a larger simple shear strain [28], as shown in Figure 5.



Figure 5: Final products of solid-state recycling of AA6061-T4 alloy recycled chips.

3. Results and Discussion

The study involved conducting tests on recycled industrial AA6061 chips. These chips were subjected to a process of hot extrusion followed by ECAP using two routes. The subsequent sections of this work elaborate on the outcomes and conclusions drawn from this experiment.

3.1. Influence of Routes on tensile strength

All specimens, including the original extruded and ECAPed AA6061-T4 specimens, had their tensile characteristics evaluated using a universal machine (SANTAM STM-50). Utilizing an electro-discharge machining EDM wire cutting apparatus, all specimens were precisely sectioned as depicted in Figure 6. Specimens with a tapered configuration were then obtained, featuring a 3 mm thickness and a 5 mm gauge length.

These samples had been clipped along the lengthwise orientation aligned with the direction of extrusion, as illustrated in Figure 7. Conforming to the ASTM E8/E8M-16 standards, the sub-sized tensile specimens adhered to specifications for a 5 mm gauge length, 3 mm width at the reduced section, and around 3 mm thickness [37].

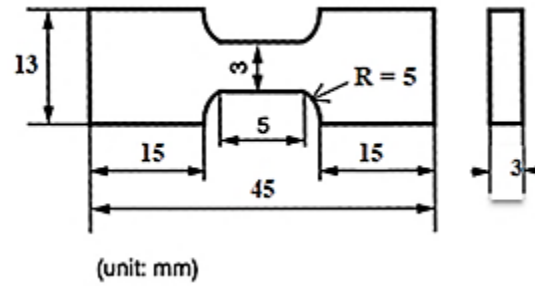


Figure 6: The dimensions of the tensile test samples are expressed in (mm).

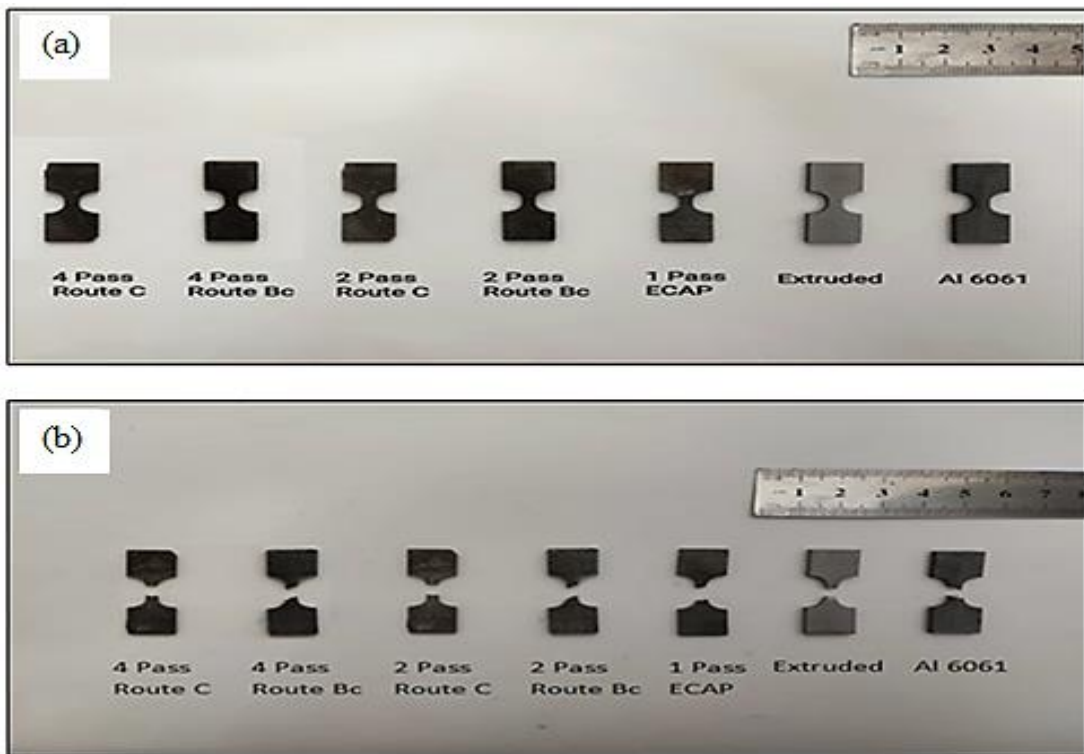


Figure 7: Representation of tensile specimens (a) specimens before tensile testing (b) specimens after tensile examination.

Tables 3 and 4 lists the mechanical properties of AA6061-T4 prior to and following processing. Extruded specimens had 33% elongation and 159 MPa, 105 MPa accordingly. With an increasing cycle number, there is a noticeable rise in both the YS and UTS numbers. After undergoing four passes, the UTS of this specimen demonstrates an enhancement to 265 MPa while the yield strength improves to 149 MPa accompanied by a remarkable elongation of 46%. While the alloy's strength improves with an increase in the number of runs, there is also a corresponding enhancement in the extent of elongation, which increases from 33 percent to 46 percent. This phenomenon can be attributed to the effects of SPD processing and its consequent strengthening through material deformation. It has been deduced that the amplified strength observed in the alloy as a result of the ECAP procedure primarily stems from the process of grain refinement [18]. Following a solitary ECAP pass, there is a notable reduction and refinement in the grain size. Moreover; the phenomenon of partition becomes evident within specific grains and along grain boundaries, and it becomes more pronounced as a consequence. Additionally; the mechanism of twinning plays a crucial role in altering the yield strength (YS) which acts as a barrier against dislocation glide and contributes to enhanced characteristics. Consequently, the increase in YS is influenced by the dual factors of grain refinement and the interplay of twinning and dislocation motion. Notably, it becomes evident that elongation is reduced after reaching a critical pass. Generally, the ductility of materials tends to decrease post-twinning. This decline in elongation can be attributed to the innate malleability of metals, while the advancement of partitioning does not significantly impact microstructure refinement.

Table 3: Mechanical properties of AA6061-T4 before and after ECAP using Route BC

Condition, Route BC	Average Hardness (HV)	Ultimate Tensile Strength (MPa)	Yield Strength (MPa)	Elongation %
As Received	81.66	250	110	27
Extruded	47.55	159	105	33
1-pass	61.16	209	135	13
2-pass	62.36	232	138	22
4-pass	79.36	265	149	46

Table 4: Mechanical properties of AA6061-T4 before and after ECAP using Route C

Condition, Route C	Average Hardness (HV)	Ultimate Tensile Strength (MPa)	Yield Strength (MPa)	Elongation %
As Received	81.66	250	110	27
Extruded	47.55	159	105	33
1-pass	61.16	209	135	13
2-pass	68.34	182	115	12
4-pass	86.06	238	136	41

Table 3 illustrates that through route BC pressing, the ultimate tensile strength (UTS) undergoes a substantial enhancement from 159 MPa to 265 MPa after undergoing four passes, marking a remarkable improvement of 67%. This enhancement in strength can be attributed to the process of grain refining, which is facilitated through repeatable passes. In contrast to the specimen that was extruded, results similarly indicate UTS rose even after just a single pass using route BC. Furthermore, as depicted in Table 4, the implementation of route C pressing results in a significant enhancement in UTS, escalating from 159 MPa to 238 MPa after undergoing four passes, indicating an impressive improvement of 50%. This strengthening effect can be attributed to the process of grain refinement facilitated by many runs. Additionally, it demonstrated that material strength experienced an exceptional increase following four passes, exhibiting a notable disparity in contrast to the extrusion one. Strengthening resulting from the

movement of dislocations and refinement of grains [38] influenced by the heightened density of dislocations due to strain strengthening. Severe plastic deformation and cold deformation bring about alterations in tensile properties of metallic strength subjected to SPD. During the initial pass, there is a marked rise, in UTS and yield strength albeit accompanied by a rapid reduction in elongation. The subsequent passes in this process yield an incremental increase in strength, fundamentally attributed to the evolving structures within the grains. Consequently, YS rates of enhancement and elongation decrease with successive passes, which are lower compared to the effects observed with the initial run.

3.2. Impact of Routes on Hardness

Tables 3 and 4 revealed a clear correlation between hardness and YS, with an elevation in YS aligning with a rise in micro-hardness. Following a single run, the YS measured 135 MPa, accompanied by a recorded hardness of 61 HV. After implementing 4 cycles, through route BC, the YS escalated to 149 MPa, and the significance hardness surged to 79 HV. Likewise; for 4 runs utilizing the same path C, the yield behavior elevated to 136 MPa, accompanied by an increased number of 86 HV.

3.3. Influence of Routes on Microstructures

The fracturing mechanisms of the fractured tension specimens have been further investigated. A 3-by-3-millimeter tip was made for each of the three separate specimens in addition to the initial specimen received to aid in this inspection. Structural testing is conducted using a SEM machine. A comprehensive analysis of the fracture properties of recycled AA6061-T4 alloy samples was carried out by examining fracture surfaces through scanning electron microscopy. Throughout the tensile tests at various stress levels 250 MPa, 159 MPa, 238 MPa, and 265 MPa fractured areas of the initial specimen

extruded in 4-runs C and the 4-runs BC samples were subjected to investigation. Observations revealed the fractures exhibited a ductile mode of propagation. Figure 8 presents the fractography images illustrating distinct fracture tendencies in recycled material alloy samples as captured by scanning electron microscopy (SEM). In Figure 8 (a), the initial specimen showcases a brittle yet also ductile fracture behavior. Conversely; Figure 8 (d) portrays the sample undergoing 4 cycles, revealing a structure resembling that of a hexagonal-cell pattern. This structural pattern is indicative of the final stages of grain refinement, implying enhanced malleability and explaining the heightened uniformity of the specimen. Furthermore; Figures 8 (b) and 8 (c) display the sample subjected to extrusion and the 4th specimen with route C, respectively. Both images illustrate specimens that display a ductile fracture tendency. Upon reaching the fourth pass of ECAP, the initial coarse grains commenced transforming into structures characterized by dislocation tangles, a transformation that considerably impacts the evolution of fracture crack behavior. The capability of cracks to propagate along dislocation walls and the boundaries of dislocation tangles leads to a modification in crack propagation direction within the larger grains. Fracture trans-granularly manifested zones of shear deformation formed in the process within the planar region, while intergranular fracturing emerged across High-Angle Grain Boundaries (HAGBs) within the granular region [39].

The escalation in the HAGBs proportion led exclusively to the propagation of intergranular fractures following the completion of four ECAP passes. Corresponding findings were documented for UFG AA6063 and AA6061 alloys after undergoing four ECAP runs [28]. On the surface morphology of UFG materials, additional secondary

cracks were also observed running parallel to the HAGBs, indicative of inter-granular cracking. Despite the fact that the four-pass pressing process of the AA6061 alloy negated the fracture enhancement observed after the two-pass ECAP, the high fracture strength of the AA6061 aluminum alloy in this investigation remained intact.

The outcomes of the present investigation showcased that the highest efficacy of fractures was attained by exposing AA6061-T4 to a sequence of 4th runs via the BC route. Most of the fracture examples conducted on processed samples have consistently exhibited this behavior, owing to the strength enhancement ECAP substantially elevating the materials' resistance against fracture. Conversely; grain refinement augments resistance against the development of fracture cracks by curbing the intensity of extrusion-induced expansions, primarily due to a reduction in the number of dislocations within slip bands. In materials treated with ECAP, the pathway for crack propagation is simplified, leading to a reduction in the propensity for crack advancement. Consequently, the enhancement of both strength and ductility plays a pivotal role in bolstering fracture resistance.

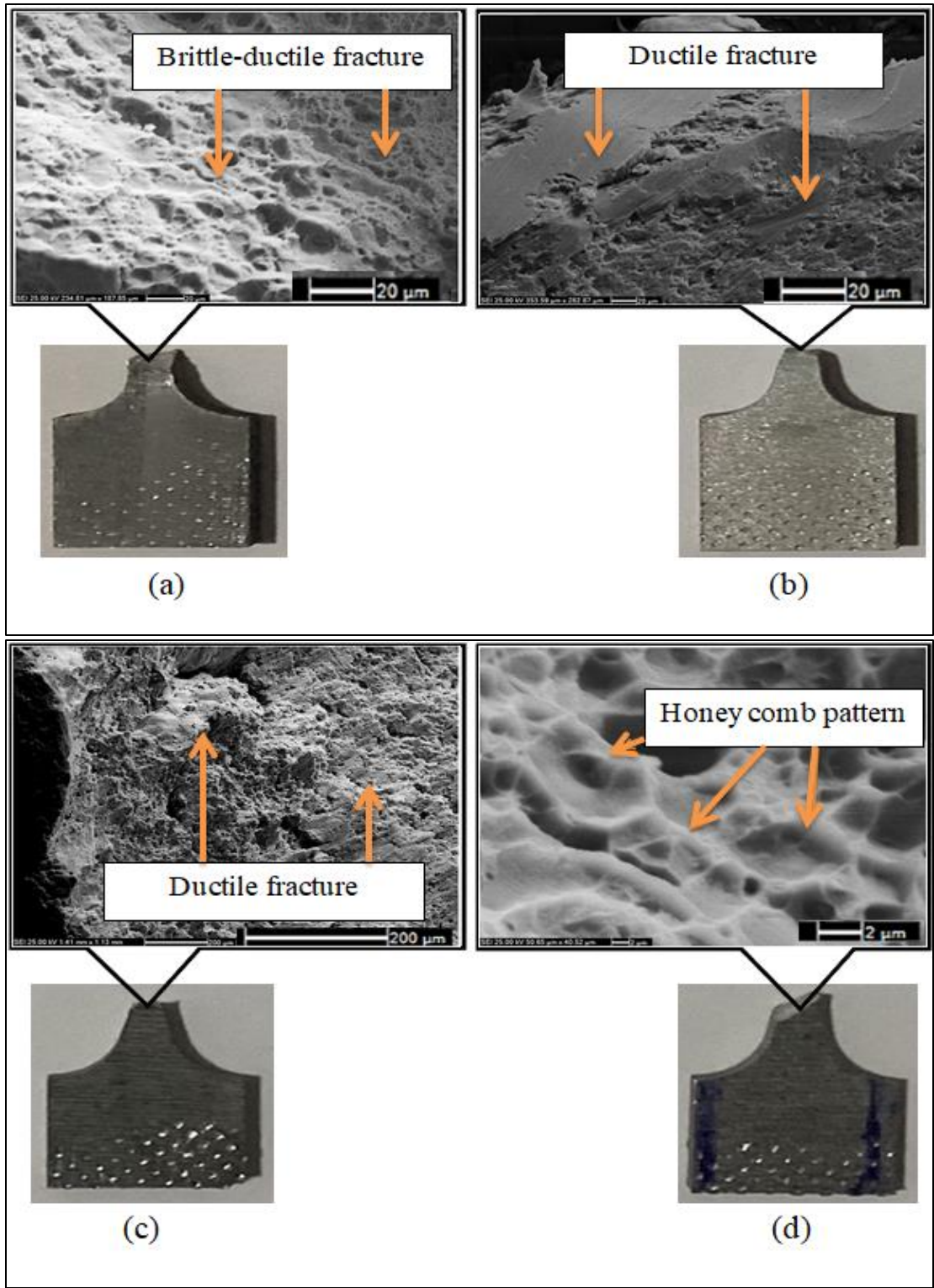


Figure 8: Different fractured specimens were seen using SEM (a) Received material brittle-ductile fracture (b) Extruded sample, (c) 4th route C ECAP specimen and (d) 4th route BC ECAP specimen displaying shear rupture.

3.4. Comparisons between the previous studies with the current study in terms of ultimate tensile strength, elongation to failure, and micro-hardness as tabulated in table 5.

Table 5: A comparisons between the previous studies with the current study in terms of ultimate tensile strength, elongation to failure, and micro-hardness.

Authors	Material	Reference	Ultimate Tensile Strength (MPa)	Elongation to failure %	Micro-Hardness (HV)	Route	Φ	Ψ	Year	Methodology
Z. Zhang et al.	AA6061	[40]	-	10.9%	-	BC	90°	30°	2018	as-cast condition ECAP
O. Abioye et al.	AA6063	[22]	-	26%	-	BC	-	-	2019	As a received ECAP
S. Kadiyan et al.	AA6063	[41]	120 MPa	9.42%	-	BC	90°	5°	2019	As a received ECAP
			176 MPa	10.95%		C				
M. Ciemiorek et al.	AA3030 Al-Mn-Fe-Si	[42]	240 MPa	-	70 HV	-	90°	-	2020	Plates as a received I-ECAP
S. Al-Alimi et al.	AA6061	[43]	245 MPa	11.9%	84 HV	-	90°	20°	2021	Boron carbide composite ECAP at 500°C
A. Gupta et al.	AA6063	[44]	250 MPa	-	80 HV	BC	120°	30°	2021	As received ECAP at 250°C
					85 HV	C				
G. Shuai et al.	AA8176 Al-Fe alloy	[45]	186 MPa	10.5%	-	BC	90°	90°	2021	As a received heat-treated at 540 °C ECAP
Current study	AA6061-T4	-	265 MPa	46%	79.6 HV	BC	90°	20°	2023	S.S.R AA chips hot extrusion followed by ECAP at RT
			238 MPa	41%	86 HV	C				

4. Conclusion

Commercial aluminum-grade AA6061-T4 chips were recycled by using hot extrusion followed by SPD processing using both routes BC, and C through the ECAP die with a 90° channel angle and 20° corner angles. The results are concluded as follows:

1. UTS demonstrated a notable escalation with an increasing number of passes. Following four passes via ECAP, both route BC and route C achieved 265 MPa and 238 MPa, respectively.
2. The findings highlighted that Route BC proved to be the most efficient pathway for generating UFG materials characterized by a uniform microstructure. Moreover, the recycling of AA6061-T4 alloy chips was found to be conducive to achieving grain refinement.
3. Examination of the fractured surfaces using scanning electron microscopy (SEM) revealed honeybee-type patterns (indicative of high ductility) after ECAP via route BC, whereas the initial specimen exhibited mixed brittle-ductile fractures.
4. The fractured sample subjected to "ECAP," particularly the Route BC sample, displayed a fracture pattern reminiscent of shear rupture resulting from tensile forces. This fracture behavior was attributed to the grain morphology and the presence of elongated dislocation cells.

5. References

- [1] P. J. I. S. R. N. Mukhopadhyay, "Alloy designation, processing, and use of AA6XXX series aluminium alloys," vol. 2012, 2012.
- [2] J. Cui, A. Kvithyld, H. J. M. Roven, Metals, and C. D. Materials Society/AIME, P. O. Box 430 Warrendale PA 15086 USA.. 14-18 Feb, "Degreasing of aluminium turnings and implications for solid-state recycling," Minerals, Metals and Materials Society/AIME, 420 Commonwealth Dr., P. O. Box ..., 2010.
- [3] B. Wan, W. Chen, T. Lu, F. Liu, Z. Jiang, M. J. R. Mao, Conservation, and Recycling, "Review of solid state recycling of aluminum chips," vol. 125, pp. 37-47, 2017.
- [4] A. Aslan, O. S. Sahin, E. Salur, A. Gunes, A. Akdemir, H. B. J. J. o. S. U. N. Karadag, and A. Science, "A new method for recycling of metal chips," vol. 4, no. 1, pp. 1-12, 2015.
- [5] Y. Estrin, and A. J. A. m. Vinogradov, "Extreme grain refinement by severe plastic deformation: A wealth of challenging science," vol. 61, no. 3, pp. 782-817, 2013. . <https://doi.org/10.1016/j.actamat.2012.10.038>
- [6] R. Z. Valiev, and T. G. J. P. i. m. s. Langdon, "Principles of equal-channel angular pressing as a processing tool for grain refinement," vol. 51, no. 7, pp. 881-981, 2006. <https://doi.org/10.1016/j.pmatsci.2006.02.003>
- [7] A. P. Zhilyaev, and T. G. J. P. i. M. s. Langdon, "Using high-pressure torsion for metal processing: Fundamentals and applications," vol. 53, no. 6, pp. 893-979, 2008. <https://doi.org/10.1016/j.pmatsci.2008.03.002>
- [8] L. Zaharia, R. Chelariu, R. J. M. S. Comaneci, and E. A, "Multiple direct extrusion: A new technique in grain refinement," vol. 550, pp. 293-299, 2012. <https://doi.org/10.1016/j.msea.2012.04.074>
- [9] H. Alihosseini, M. A. Zaeem, K. Dehghani, and H. A. J. M. L. Shivaee, "Producing ultrafine-grained aluminum rods by cyclic forward-backward extrusion: Study the microstructures and mechanical properties," vol. 74, pp. 147-150, 2012. <https://doi.org/10.1016/j.matlet.2012.01.102>
- [10] L. Su, C. Lu, A. K. Tieu, G. Deng, X. J. M. S. Sun, and E. A, "Ultrafine grained AA1050/AA6061 composite produced by accumulative roll bonding," vol. 559, pp. 345-351, 2013. <https://doi.org/10.1016/j.msea.2012.08.109>
- [11] E. Tan, A. A. Kibar, and C. H. J. M. C. Gür, "Mechanical and microstructural characterization of 6061 aluminum alloy strips severely deformed by dissimilar channel angular pressing," vol. 62, no. 4, pp. 391-397, 2011. <https://doi.org/10.1016/j.matchar.2011.01.016>
- [12] K. O. Sanusi, O. D. Makinde, and G. J. J. S. A. J. o. S. Oliver, "Equal channel angular pressing technique for the formation of ultra-fine grained structures," vol. 108, no. 9, pp. 1-7, 2012. <https://hdl.handle.net/10520/EJC127477>
- [13] R. Z. Valiev, I. Sabirov, A. P. Zhilyaev, and T. G. J. J. Langdon, "Bulk nanostructured metals for innovative applications," vol. 64, pp. 1134-1142, 2012. <https://doi.org/10.1007/s11837-012-0427-9>
- [14] J. R. Duflou, A. E. Tekkaya, M. Haase, T. Welo, K. Vanmeensel, K. Kellens, W. Dewulf, and D. J. C. A. Paraskevas, "Environmental assessment of solid state recycling routes for aluminium alloys: can solid state processes significantly

- reduce the environmental impact of aluminium recycling?,” vol. 64, no. 1, pp. 37-40, 2015. <https://doi.org/10.1016/j.cirp.2015.04.051>
- [15] D. Baffari, G. Buffa, D. Campanella, and L. J. P. M. Fratini, “Design of continuous Friction Stir Extrusion machines for metal chip recycling: issues and difficulties,” vol. 15, pp. 280-286, 2018. <https://doi.org/10.1016/j.promfg.2018.07.220>
- [16] W. Maziarz, M. Greger, P. Długosz, J. Dutkiewicz, A. Wójcik, Ł. Rogal, K. Stan-Głowińska, O. Hilser, M. Pastrnak, L. J. J. o. M. R. Cizek, and Technology, “Effect of severe plastic deformation process on microstructure and mechanical properties of AlSi/SiC composite,” 2022. <https://doi.org/10.1016/j.jmrt.2022.01.023>
- [17] K. M. Agarwal, R. Tyagi, V. Choubey, K. K. J. A. i. M. Saxena, and P. Technologies, “Mechanical behaviour of Aluminium Alloy AA6063 processed through ECAP with optimum die design parameters,” pp. 1-15, 2021. <https://doi.org/10.1016/j.matpr.2021.03.681>
- [18] M. Baig, A. U. Rehman, J. A. Mohammed, and A. H. J. C. Seikh, “Effect of microstructure and mechanical properties of Al5083 alloy processed by ECAP at room temperature and high temperature,” vol. 11, no. 6, pp. 683, 2021. <https://doi.org/10.3390/cryst11060683>
- [19] P. C. Gautam, S. J. M. S. Biswas, and E. A, “On the possibility to reduce ECAP deformation temperature in magnesium: Deformation behaviour, dynamic recrystallization and mechanical properties,” vol. 812, pp. 141103, 2021. <https://doi.org/10.1016/j.msea.2021.141103>
- [20] M. Lefstad, K. Pedersen, S. J. M. S. Dumoulin, and E. A, “Up-scaled equal channel angular pressing of AA6060 and subsequent mechanical properties,” vol. 535, pp. 235-240, 2012. <https://doi.org/10.1016/j.msea.2011.12.073>
- [21] M. I. J. J. o. M. R. Abd El Aal, and Technology, “The influence of ECAP and HPT processing on the microstructure evolution, mechanical properties and tribology characteristics of an Al6061 alloy,” vol. 9, no. 6, pp. 12525-12546, 2020. <https://doi.org/10.1016/j.jmrt.2020.08.099>
- [22] O. Abioye, P. Atanda, G. Osinkolu, A. Abioye, I. Olumor, O. Odunlami, and S. J. P. M. Afolalu, “Influence of equal channel angular extrusion on the tensile behavior of Aluminum 6063 alloy,” vol. 35, pp. 1337-1343, 2019. <https://doi.org/10.1016/j.promfg.2019.05.020>
- [23] M. I. Ab Kadir, M. S. Mustapa, N. A. Latif, and A. S. J. P. E. Mahdi, “Microstructural analysis and mechanical properties of direct recycling aluminium chips AA6061/Al powder fabricated by uniaxial cold compaction technique,” vol. 184, pp. 687-694, 2017. <https://doi.org/10.1016/j.proeng.2017.04.141>
- [24] M. A. Taha, A. T. Abbas, F. Benyahia, H. F. Alharbi, B. Guitián, and X. R. J. J. o. C. Nova, “Enhanced corrosion resistance of recycled aluminum alloy 6061 chips using hot extrusion followed by ECAP,” vol. 2019, 2019. <https://doi.org/10.1155/2019/3658507>
- [25] M. I. Abd El Aal, M. A. Taha, A. Selmy, A. El-Gohry, and H. J. M. R. E. Kim, “Solid state recycling of aluminium AA6061 alloy chips by hot extrusion,” vol. 6, no. 3, pp. 036525, 2018. <https://orcid.org/0000-0002-0173-8256>

- [26] J. Liang, Z. Zhang, M. Jia, L. Cao, C. Li, H. Gao, J. Wang, D. J. M. S. Zhang, and E. A, "The microstructures and tensile mechanical properties of ultrafine grained and coarse grained Al-7Si-0.3 Mg alloy rods fabricated from machining chips," vol. 729, pp. 29-36, 2018. <https://doi.org/10.1016/j.msea.2018.05.047>
- [27] J. Gronostajski, H. Marciniak, and A. J. J. o. m. p. t. Matuszak, "New methods of aluminium and aluminium-alloy chips recycling," vol. 106, no. 1-3, pp. 34-39, 2000. [https://doi.org/10.1016/S0924-0136\(00\)00634-8](https://doi.org/10.1016/S0924-0136(00)00634-8)
- [28] M. A. Kazemi, R. J. M. S. Seifi, and E. A, "Effects of crack orientation on the fatigue crack growth rate and fracture toughness of AA6063 alloy deformed by ECAP," vol. 733, pp. 71-79, 2018. <https://doi.org/10.1016/j.msea.2018.07.042>
- [29] H. Zhang, M. Chen, K. Ramesh, J. Ye, J. Schoenung, E. J. M. S. Chin, and E. A, "Tensile behavior and dynamic failure of aluminum 6092/B4C composites," vol. 433, no. 1-2, pp. 70-82, 2006. <https://doi.org/10.1016/j.msea.2006.06.055>
- [30] T. Ramachandran, "Advances in Aluminium Processing and Its Automotive Application." pp. 28-32.
- [31] A. Selmy, A. El-Gohry, M. Abd El Aal, and M. Taha, "Characteristics of solid state recycling of aluminum alloy (AA6061) chips by hot extrusion." pp. 316-323.
- [32] Y. Iwahashi, Z. Horita, M. Nemoto, and T. G. J. A. m. Langdon, "The process of grain refinement in equal-channel angular pressing," vol. 46, no. 9, pp. 3317-3331, 1998. [https://doi.org/10.1016/S1359-6454\(97\)00494-1](https://doi.org/10.1016/S1359-6454(97)00494-1)
- [33] T. G. J. M. S. Langdon, and E. A, "The principles of grain refinement in equal-channel angular pressing," vol. 462, no. 1-2, pp. 3-11, 2007. <https://doi.org/10.1016/j.msea.2006.02.473>
- [34] A. Vinogradov, S. Yasuoka, and S. Hashimoto, "On the effect of deformation mode on fatigue: simple shear vs. pure shear." pp. 797-802. <https://doi.org/10.4028/www.scientific.net/MSF.584-586.797>
- [35] P. B. Berbon, M. Furukawa, Z. Horita, M. Nemoto, T. G. J. M. Langdon, and M. T. A, "Influence of pressing speed on microstructural development in equal-channel angular pressing," vol. 30, pp. 1989-1997, 1999. <https://doi.org/10.1007/s11661-999-0009-9>
- [36] R. Valiev, and T. J. c. a. p.-i. a. a. p. t. f. g. r. Langdon, "Principles of equal," Progress in Materials Science, 2006, pp. 881-981.
- [37] A. J. W. C. A. I. Standard, "E8/E8M-16a standard test methods for tension testing of metallic materials," 2016.
- [38] M. Abbasi-Baharanchi, F. Karimzadeh, M. J. M. S. Enayati, and E. A, "Mechanical and tribological behavior of severely plastic deformed Al6061 at cryogenic temperatures," vol. 683, pp. 56-63, 2017. <https://doi.org/10.1016/j.msea.2016.11.099>
- [39] A. J. J. o. m. s. Vinogradov, "Fatigue limit and crack growth in ultra-fine grain metals produced by severe plastic deformation," vol. 42, pp. 1797-1808, 2007. <https://doi.org/10.1007/s10853-006-0973-z>
- [40] Z. Zhang, J. Wang, Q. Zhang, S. Zhang, Q. Shi, and H. J. M. Qi, "Research on grain refinement mechanism of 6061 aluminum alloy processed by combined SPD methods of ECAP and MAC," vol. 11, no. 7, pp. 1246, 2018. <https://doi.org/10.3390/ma11071246>

- [41] S. Kadiyan, and B. J. M. R. E. Dehiya, "Evaluating the influence of various routes on micro-structure and mechanical properties of AA-6063 after equal channel angular pressing," vol. 6, no. 8, pp. 0865f9, 2019. <https://orcid.org/0000-0002-2163-1915>
- [42] M. Ciemiorek, M. Lewandowska, L. J. M. Olejnik, and Design, "Microstructure, tensile properties and formability of ultrafine-grained Al–Mn square plates processed by Incremental ECAP," vol. 196, pp. 109125, 2020. <https://doi.org/10.1016/j.matdes.2020.109125>
- [43] S. Al-Alimi, M. A. Lajis, S. Shamsudin, N. K. Yusuf, B. Chan, D. D. Hissein, M. H. Rady, M. S. Msebawi, H. M. J. M. Sabbar, and Technology, "Hot extrusion followed by a hot ecap consolidation combined technique in the production of boron carbide (B4C) reinforced With aluminium chips (AA6061) composite," vol. 55, no. 3, pp. 347–354-347–354, 2021. <https://doi.org/10.17222/mit.2020.177>
- [44] A. Gupta, K. Saxena, A. Bharti, J. Lade, K. Chadha, P. R. J. A. i. M. Paresi, and P. Technologies, "Influence of ECAP processing temperature and number of passes on hardness and microstructure of Al-6063," pp. 1-12, 2021. <https://doi.org/10.1080/2374068X.2021.1953917>
- [45] G. Shuai, Z. Li, D. Zhang, Y. Tong, and L. J. V. Li, "The mechanical property and electrical conductivity evolution of Al–Fe alloy between room temperature and elevated temperature ECAP," vol. 183, pp. 109813, 2021. <https://doi.org/10.1016/j.vacuum.2020.109813>